Alzheimer's & Dementia®
THE JOURNAL OF THE ALZHEIMER'S ASSOCIATION

RESEARCH ARTICLE

Retinal vascular alterations in cognitive impairment: A multicenter study in China

Qin Shi[1] | Andrew Ni[2,3] | Kexin Li[2] | Wenxin Su[2,4] | Wenbin Xie[2] | Hao Zheng[2] | Mingxuan Wang[5] | Zhenxu Xiao[6,7,8] | Wanqing Wu[6,7,8] | Kaiwen Shi[2] | Peijun Zhang[2] | Biao Yan[2] | Ding Ding[6,7,8] | Timothy Kwok[9] | Qianhua Zhao[6,7,8] | Jiayi Zhang[2]

[1]Department of Ophthalmology, General Hospital of Ningxia Medical University, Yinchuan, China

[2]Institutes of Brain Science, State Key Laboratory of Medical Neurobiology, MOE Frontiers Center for Brain Science, Institute for Medical and Engineering Innovation, Department of Ophthalmology, Eye & ENT Hospital, Fudan University, Shanghai, China

[3]Warren Alpert Medical School, Brown University, Providence, Rhode Island, USA

[4]Department of Psychology, University of Essex, Wivenhoe Park, Colchester, UK

[5]Department of Biomedical Engineering, Johns Hopkins University, Wyman Park Building, Baltimore, Maryland, USA

[6]Institute of Neurology, Huashan Hospital, Fudan University, Jing'an, Shanghai, China

[7]National Clinical Research Center for Aging and Medicine, Huashan Hospital, Fudan University, Jing'an, Shanghai, China

[8]National Center for Neurological Disorders, Huashan Hospital, Fudan University, Jing'an, Shanghai, China

[9]Department of Medicine & Therapeutics, Prince of Wales Hospital, The Chinese University of Hong Kong, Shatin, New Territories, Hong Kong SAR

Correspondence
Qianhua Zhao, Institute of Neurology, Huashan Hospital, Fudan University, 12 Wulumuqi Middle Road, Jing'an, Shanghai 200040, China.
Email: qianhuazhao@fudan.edu.cn

Timothy Kwok, Department of Medicine & Therapeutics, Prince of Wales Hospital, The Chinese University of Hong Kong, 30-32 Ngan Shing Street, Shatin, New Territories, Hong Kong SAR.
Email: tkwok@cuhk.edu.hk

Jiayi Zhang, Institutes of Brain Science, State Key Laboratory of Medical Neurobiology, MOE Frontiers Center for Brain Science, Department of Ophthalmology, Eye and ENT Hospital, 131 Dong'an Road, Fudan University, Xuhui, Shanghai 200032, China.
Email: jiayizhang@fudan.edu.cn

Abstract

INTRODUCTION: Foundational models suggest Alzheimer's disease (AD) can be diagnosed using retinal images, but the specific structural features remain poorly understood. This study investigates retinal vascular changes in individuals with cognitive impairment in three East Asian regions.

METHODS: A multicenter study was conducted in Shanghai, Hong Kong, and Ningxia, collecting retinal images from 176 patients with mild cognitive impairment (MCI) or AD and 264 controls. The VC-Net deep learning model segmented arterial/venous networks, extracting 36 vascular features.

RESULTS: Significant reductions in vessel length, segment number, and vascular density were observed in cognitively impaired patients, while venous structure and complexity were correlated with the level of cognitive function.

DISCUSSION: Retinal vascular changes may serve as indicators of cognitive impairment, requiring validation in larger cohorts and exploration of the underlying mechanisms.

KEYWORDS
Alzheimer's disease, cognitive impairment, early biomarkers, interpretable deep learning, retinal imaging, vascular structure

Highlights
- A deep learning segmentation model extracted diverse retinal vascular features.
- Significant alterations in the structure of retinal arterial/venous networks were identified.
- Partitioning vessel-rich retinal zones improved detection of vascular changes.
- Decreases in vessel length, segment number, and vascular density were found in CI individuals.

1 | INTRODUCTION

Traditionally, diagnosing Alzheimer's disease (AD) and other forms of dementia relies on a combination of medical history, neurological exams, cognitive assessments, and neuroimaging techniques like magnetic resonance imaging (MRI) and positron emission tomography (PET) scans.[1] Amyloid PET imaging and the measurement of amyloid and tau deposits in cerebrospinal fluid (CSF) or blood have become increasingly accepted in diagnostic practices, supported by clinical evidence.[2–4] However, these methods are often invasive, costly, and resource-intensive, limiting their practicality for widespread screening. According to the World Alzheimer Report 2022, approximately 75% of individuals with dementia remain undiagnosed globally. This percentage is estimated to climb even higher, potentially reaching up to 90% in some low- and middle-income nations.[5] Notably, over half of the global dementia population is expected to reside in Asia by 2050,[6] despite Asians being historically underrepresented in dementia research and typically constituting less than 3% of participants in major AD datasets.[7,8] Thus, there exists an urgent need for cost-effective and efficient diagnostic tools for detecting and monitoring cognitive impairment, especially in East Asia.

Pathological changes, predominantly related to AD like amyloid-beta plaques and tau neurofibrillary tangles, often progress slowly and can remain undetected for years.[9] Identifying these changes when cognitive symptoms are mild or emerging is crucial for timely intervention and slowing disease progression. The retina, as an extension of the central nervous system, offers a unique, non-invasive window into microvascular health and brain-related pathology.[10–12] Previous studies have shown patients with mild cognitive impairment (MCI) and AD exhibit reduced arteriovenous differences in oxygen saturation, retinal blood flow, and arterial vessel diameter.[13] In addition, Asanad et al. found changes in retinal nerve fiber layer thickness were able to predict individuals with CSF biomarkers indicative of AD pathology before the onset of symptomatic cognitive impairment.[14] These findings suggest various retinal imaging technologies hold promise in monitoring or detecting cognitive impairment and its associated pathophysiological changes.

Recent studies have also suggested retinal vascular features may serve as valuable biomarkers for cognitive impairment and related neurological conditions.[15] Structural optical coherence tomography (OCT) imaging can reveal hyperreflective deposits in AD associated with disruptions in the outer retina, while OCT angiography (OCTA) can detect microvascular alterations in AD patients, potentially serving as valuable criteria for differential diagnosis.[16–18] These findings support the potential of retinal imaging as a viable and accessible option for conducting large-scale screening initiatives, particularly in resource-constrained communities.[19]

Digital retinal fundus imaging remains a low-cost, easily accessible technique in primary care settings that can capture retinal vascular features. It offers a comprehensive view of the retina and detailed structural information that complements OCT data, particularly when assessing overall retinal vascular structures.[20,21] Cheung et al. conducted a proof-of-concept study to illustrate the validity of using a deep learning model in detecting AD using retinal fundus images.[22] The study concluded that an unsupervised domain adaptation deep learning technique using retinal fundus images alone can detect AD in diverse clinical populations with common risk factors and comorbidities such as diabetes, hypertension, and other concomitant eye diseases. Zhou et al. took this a step further and pretrained a foundational deep learning model using 1.6 million retinal images finetuned to detect various diseases.[23] These deep learning models have demonstrated the feasibility of learning the discriminative features from retinal images for detecting AD and cognitive impairment, but what these discriminative features are, and their underlying physiological or pathological interpretations remain poorly understood.

Here, we aimed to identify statistically significant alterations in retinal vascular features extracted from fundus images of normal cognitive (NC) individuals compared to those cognitively impaired (CI) including MCI and AD across three medical centers in China. Notably, we used an interpretable deep learning model to segment and analyze vascular features in these images. By comparing NC and CI groups, we aimed to uncover specific retinal vascular changes, including diameters, densities, and number of bifurcation points, that may be correlated with the degree of cognitive impairment.

2 | METHODS

2.1 | Participants and data acquisition

We recruited study participants from Huashan Hospital in Shanghai, Prince of Wales Hospital in Hong Kong, and General Hospital of Ningxia Medical University in Yinchuan. Inclusion criteria were as follows: (1) aged ≥ 65 years; (2) cooperated to physical examinations, neuropsychological tests, and retinal fundus imaging; and (3) had detailed medical records of clinical data. Exclusion criteria included: (1) history of psychiatric disorders or dementia due to Lewy body disease, Parkinson's disease, frontotemporal lobar degeneration, traumatic brain injury, or multiple sclerosis; (2) history of ophthalmological disorders including age-related macular degeneration, retinal vascular disease such as hypertensive or diabetic retinopathy, glaucoma, or increased intraocular pressure, severe myopia, optic neuropathy, or other optic nerve disorders and anterior segment diseases such as ocular trauma or cataract that interfered with the fundus examination; and (3) retinal fundus imaging did not pass quality examination.

The cognitive function of each participant was determined by a neurologist based on neurological symptoms, cognitive performance (including Montreal Cognitive Assessment (MoCA), Mini-Mental State Examination (MMSE), and other domain-specific neuropsychological tests), activities of daily living, and medical histories. The presence or absence of dementia was defined by Diagnostic and Statistical Manual of Mental Disorders, Fourth Edition (DSM-IV) criteria,[24] while AD was diagnosed with National Institute of Neurological and Communicative Disorders and Stroke and Alzheimer's Disease and Related Disorders Association (NINCDS-ADRDA) criteria.[25] Only those who were not diagnosed with dementia were considered for a diagnosis of MCI based on Petersen's criteria.[26] Study participants were further separated into two groups, NC and CI, which included MCI and AD. Those given a probable or possible AD diagnosis according to the NINCDS-ADRDA criteria have a 91% rate of *post mortem* pathological confirmation of AD with 83% sensitivity and 84% specificity.[27,28]

This study was approved by the Joint Chinese University of Hong Kong-New Territories East Cluster Clinical Research Ethics Committee, General Hospital of Ningxia Medical University, and the Medical Ethics Committee of Huashan Hospital, Fudan University, Shanghai. Informed consent was obtained from all participants. For each participant, macula-centered fundus images were captured in a dark room (with all lights off) without pupillary dilation using different imaging devices at the three study centers. In Huashan Hospital, Shanghai, images were captured using the AFC-330 (NIDEK). In the General Hospital of Ningxia Medical University, images were captured using the CLARUS500 (ZEISS). In the Prince of Wales Hospital in Hong Kong, images were captured using the TRC-NW400 (TOPCON). The imaging procedures were carried out by experienced technicians, ensuring consistency, and accuracy across all sites. Only images that passed quality examination of two physicians were included in this study.

RESEARCH IN CONTEXT

1. **Systematic review**: We conducted a thorough literature review on retinal imaging and Alzheimer's disease (AD), suggesting an association of fundus vascular changes with AD. Developments in deep learning highlight retinal fundus imaging as a non-invasive alternative, reflecting AD pathology through changes in specific structures in the retinal vasculature.
2. **Interpretation**: Our study identifies specific retinal vascular changes in patients with mild cognitive impairment (MCI) and AD using retinal fundus imaging. We observed significant differences in vascular density, length, and morphology between normal cognitive (NC) and cognitively impaired (CI) individuals. These changes may serve as early biomarkers for cognitive impairment.
3. **Future directions**: Future research should validate these findings in larger, diverse cohorts and explore mechanisms linking structural vasculature changes to AD in longitudinal studies. Investigating regional retinal differences and accounting for comorbidities may enhance AD detection and monitoring.

2.2 | Retinal vessel segmentation

Retinal vessel segmentation identifies and isolates the vasculature within the original retinal fundus images, producing binary images that exclusively represent the blood vessels while excluding any extraneous retinal information.[29] Various vascular features are calculated based on these binary vessel images. Previous studies that identified retinal vascular biomarkers for early detection of AD found biomarkers related not only to overall retinal blood vessels but also to retinal arteries and veins separately.[30,31] Consequently, to accurately identify these retinal arteries and veins, a deep learning model called VC-Net was used and adjusted in this study.[32,33] This model was trained on the DRIVE-AV dataset, which consists of 40 retinal fundus images annotated to distinguish arteries and veins. The model produces three binary vessel images, corresponding to all vessels, arterial vessels, and venous vessels.

Although VC-Net achieves high accuracy in vessel segmentation, it is important to note that the classification of arteries and veins can sometimes be challenging due to the complex and diverse structures of blood vessels. For example, as shown in the green areas of Figure 1A, the occasional overlapping of arteries and veins may make separation difficult. Furthermore, microvessels on the tail end of vessel branches are also challenging to recognize. To address this, in addition to analyzing retinal vascular structures as a whole, two zones were also partitioned from the full fundus images to analyze vessel-rich areas, as depicted in Figure 1B. Starting from the center of the optic disc, Zone B is the area
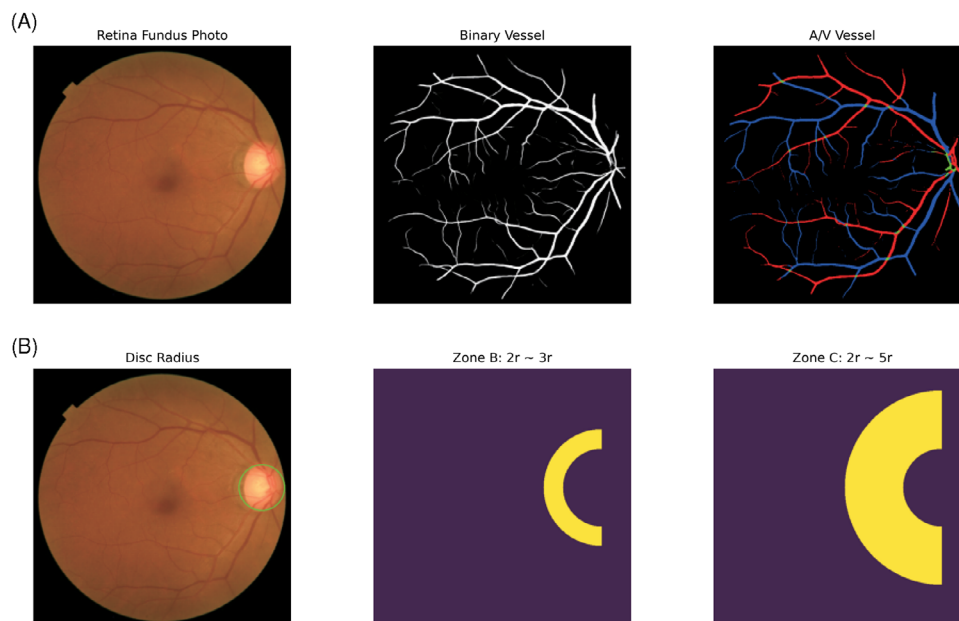
FIGURE 1 Example images of retinal vessel segmentation and zone division of retinal vascular area. (A) Left, original retinal fundus image; middle, binary vessel image; right, binary segmentation of arteries and veins. Red: arteries. Blue: veins. Green: overlaps of arteries and veins. (B) Left, the radius of the optic disc is used as a unit to define areas of the retinal fundus image; middle, Zone B is the area 2x to 3x radii away from the disc margin; right, Zone C is the area 2x to 5x radii away from the disc margin.

between 2x and 3x the optic disc radius and Zone C is the area between 2x and 5x the optic disc radius (Figure 1B).

2.3 | Feature extraction

Drawing from prior research on biomarkers associated with AD,[32,34] we selected features to characterize vessel richness, distribution, and morphology across distinct retinal zones. All extracted features and their corresponding abbreviations can be found in Table 1.

The calculation of density is determined by the count of pixels corresponding to all vessels on the image, with all images standardized to the same size. This measurement assesses the overall area occupied by the vasculature in the retinal image. Skeleton_len represents the number of pixels in the skeletonized representation of the fundus image, which is a measure of the extent of the vascular network while considering the reduced vessel width. N_cross indicates the number of points where the skeletonized vascular tree splits into smaller branches. Counting the number of bifurcation points provides an indicator of the morphological richness or complexity of the vessel network.

The number of vessel segments and the skeleton length are characterized for Zone B and Zone C, respectively. After calculating the diameter of each skeletonized pixel for each vessel segment, the mean and standard deviation of the diameter are then computed as Zb_width, Zb_width_std, Zc_width, and Zc_width_std. In addition, the fractal dimension in Zone C is calculated separately, characterizing the distribution of vessel density in Zone C. Utilizing vascular segmentation images of veins, arteries, and all vessels, the aforementioned 12

features are computed three times. Therefore, a total of 36 vascular features are extracted from the original retinal fundus images.

2.4 | Statistical analysis

Statistical analysis of retinal vascular features in both NC and CI (MCI and AD) patients was carried out using *R* (v4.3.2) and *Python* (v3.10.6). Demographic variables were compared using the chi-squared test for categorical variables (gender, hypertension, and diabetes) and analysis of variance (ANOVA) for continuous variables (age, education) via scipy (v1.12.0) ($p < 0.05$ considered significant).

To account for confounding demographic variables including age, education, gender, hypertension, and diabetes, a multivariate general linear model (GLM) was employed for analysis of covariance (ANCOVA) of each vascular feature between the NC and CI groups using rstatix (v0.7.2). This adjustment allowed for comparison of group variances while adjusting for confounders. For comparison between features, effect sizes were calculated as partial eta-squared with 0.01 being small, 0.06 being medium, and 0.14 being large effect sizes. Partial eta-squared (η_p^2) is the proportion of variance in a dependent variable explained by a specific independent variable while accounting for confounders. To minimize the likelihood of false-positive results, we adjusted the *p*-values using the Benjamini-Hochberg false discovery rate (FDR) method using statsmodels (v0.13.2). *p*-values were adjusted separately for left and right eyes as the underlying data for each eye was different and the sample sizes were different due to exclusion criteria (left = 363, right = 390). To achieve a balance between discovery and false positive rates, we selected an FDR (Q-value) threshold

TABLE 1 Extracted retinal vascular features.

Parameter	Retinal vascular feature	Abbreviation
Overall	Total density of retinal fundus blood vessels	Density
	Total length of retinal fundus blood vessels	Skeleton_len
	Total number of bifurcation points of retinal fundus blood vessels	N_cross
	Total density of retinal fundus arteries	DensityA
	Total length of retinal fundus arteries	Skeleton_lenA
	Number of bifurcation points of retinal fundus arteries	N_crossA
	Total density of retinal fundus veins	DensityV
	Total length of retinal fundus veins	Skeleton_lenV
	Number of bifurcation points of retinal fundus veins	N_crossV
Zone B	Number of effective vascular segments in Zone B	Zb_num
	Total length of blood vessels in Zone B	Zb_len
	Average diameter of blood vessels in Zone B	Zb_width
	Standard deviation of diameters of blood vessels in Zone B	Zb_width_std
	Number of effective arterial segments in Zone B	Zb_numA
	Total length of arteries in Zone B	Zb_lenA
	Average diameter of arteries in Zone B	Zb_widthA
	Standard deviation of diameters of arteries in Zone B	Zb_width_std
	Number of effective venial segments in Zone B	Zb_numV
	Total length of veins in Zone B	Zb_lenV
	Average diameter of veins in Zone B	Zb_widthV
	Standard deviation of diameters of veins in Zone B	Zb_width_stdV
Zone C	Number of effective vascular segments in Zone C	Zc_num
	Total length of blood vessels in Zone C	Zc_len
	Average diameter of blood vessels in Zone C	Zc_width
	Standard deviation of diameters of blood vessels in Zone C	Zc_width_std
	Fractal dimension of blood vessels in Zone C	Zc_fd
	Number of effective arterial segments in Zone C	Zc_numA
	Total length of arteries in Zone C	Zc_lenA
	Average diameter of arteries in Zone C	Zc_widthA
	Standard deviation of diameters of arteries in Zone C	Zc_width_std
	Fractal dimension of arteries in Zone C	Zc_fdA
	Number of effective venial segments in Zone C	Zc_numV
	Total length of veins in Zone C	Zc_lenV
	Average diameter of veins in Zone C	Zc_widthV
	Standard deviation of diameters of veins in Zone C	Zc_width_stdV
	Fractal dimension of veins in Zone C	Zc_fdV

of 0.1. Retinal vascular features were compared for the left and right eyes separately to mitigate potential participant-specific correlations and identify the most robust alterations in the retinal vasculature. For the comparison between three groups, we performed ANCOVA analysis as described above. We stratified the patients into three groups, NC (MoCA > 25), MCI (MoCA 19-25), and severe dementia (SD, MoCA < 18) using MoCA scores. P-values were first adjusted using Tukey post-hoc after ANCOVA for multiple comparisons between the three groups. Then, these pairwise *p*-values were further adjusted using the Benjamini-Hochberg method for the left and right eyes separately. Estimated marginal means, also known as covariate-adjusted means, were obtained using emmeans (v1.10.2).

To explore the association between retinal vascular features and cognitive performance (MoCA scores), we performed GLM regression analyses for each feature while including age, education, gender, hypertension, and diabetes as covariates using statsmodels (v0.13.2). We did

not construct a single model for all the vascular features as they all come from the same underlying data and have high multicollinearity. Separate models were constructed for the left and right eye features. Each model was fitted twice, once with unstandardized variables to obtain the regression coefficients and once with z-scored variables to obtain beta coefficients which can be compared between models. To minimize the likelihood of false positives due to multiple hypothesis testing, we performed the same p-value adjustment procedure as above. We chose to use MoCA scores as opposed to MMSE scores as it is considered a better measure of cognitive function due to its superior detection of cognitive heterogeneity (MCI especially) and lack of ceiling effect.[35,36]

To visualize significant retinal features, we calculated their pairwise Pearson correlation coefficients using scipy (v1.12.0). We also performed hierarchical clustering on the heatmap to identify similar features. The heatmap was ordered using the order of features in the dendrogram with a cutoff at 1 for clustering. Volcano plots were generated to visualize the magnitude and significance of changes, with log2 fold changes on the x-axis and -log10 Q-values on the y-axis. Dots that are higher and further to the sides represent more significant features in the volcano plot. All plots were generated using seaborn (v0.11.0).

2.5 | Classification models

To evaluate the effectiveness of the identified vascular features in distinguishing between NC and CI individuals, we conducted classification analyses using logistic regression, support vector machine (SVM), and random forest models from scikit-learn (1.4.2). Data from both eyes were combined for classification. Each model was trained using different sets of features: demographics alone, significant vascular features alone (Q-value < 0.05), a combination of demographics and vascular features, DINOv2 features alone, and a combination of demographics and DINOv2 features. DINOv2 (self-distillation with no labels version 2) is a self-supervised learning technique to train deep learning models.[37] We used a pretrained DINOv2 model (specifically, 'dinov2_vitb14_reg') to embed retinal fundus images into a 768 dimension feature space.[38] DINOv2 models can transform images into features that can be directly used by classifiers as simple as linear layers on various classification tasks. The extracted features are typically robust and perform well across domains without the need for fine-tuning. These features served as uninterpretable deep-learning features that we could compare the performance of in contrast to our identified vascular features.

To avoid data leakage between pairs of patients and to obtain more reliable metrics, we performed five-fold cross-validation using *StratifiedGroupKFold* on patient IDs. This ensured a patient with data from both the left and right eye ended up fully in the train or test set and not split up. Classification performance metrics, including accuracy, area under the receiver operating characteristic (ROC) curve (AUC), and Brier score were calculated for each fold using scikit-learn (1.4.2). The 95% confidence intervals were calculated using the standard error from the folds. The Brier score is a strictly proper scoring

rule unlike accuracy that takes into account the accuracy of the probabilities predicted by the models. This is a useful metric for diagnostic and screening tools as different users may have different risk thresholds for action. A lower Brier score is better with 0 being the best score and 1 being the worst.

3 | RESULTS

3.1 | Multicenter clinical characteristics

In total, 440 individuals participated in the study across three medical centers including Huashan Hospital in Shanghai, Prince of Wales Hospital in Hong Kong, and General Hospital of Ningxia Medical University in Yinchuan, including 264 NC individuals and 176 with MCI or AD, collectively categorized as the CI group. The demographic characteristics of the study participants are shown in Table 2. Relevant comorbid medical conditions with known impact on the retinal vasculature included hypertension and diabetes. No significant differences in age ($p = 0.256$), gender ($p = 0.586$), or diabetes prevalence ($p = 0.368$) were found between NC and CI groups. However, the CI group exhibited a significantly lower prevalence of hypertension ($p = 0.042$) and a significantly lower number of years of education ($p = 0.003$).

Due to the exclusion criteria, not all participants provided fundus images for both eyes. Thus, 363 images of left eyes (222 from NC and 141 from CI) and 390 images of right eyes (237 from NC and 153 from CI) were used for the final analysis. To accurately extract retinal vascular features for comparison between CI and NC groups, we modified a deep learning model called VC-Net to segment retinal arteries and veins. In total, 36 retinal vascular features were extracted by binarizing the identified vessels (Figure 1A, middle) to calculate vessel density and skeletonizing them to calculate crossing points and vessel length (Figure 2A). The skeleton was segmented based on crossing points, and the width of each segment was calculated (Figure 2B). Additionally, we analyzed two subzones within the fundus images: Zone B and Zone C (Figure 1B and 2C).

3.2 | Significant differences between NC and CI groups

ANCOVA analysis adjusted for age, education, gender, hypertension, and diabetes revealed significant differences in various retinal vascular features between the CI and NC groups. After FDR adjustment, 7 features in the left eye and 15 in the right eye showed significant changes (Q-value < 0.1). In the overall fundus images, the CI group demonstrated notable reductions in the total density and total length of both retinal arteries and veins compared to the NC group (densityA, densityV, skeleton_lenA, skeleton_lenV) (Figure 2). Although the total number of retinal vascular bifurcation points (n_cross, Figure 2H) significantly increased overall, the total number of retinal venous bifurcation points (n_crossV, Figure 2I) in

TABLE 2 Demographic characteristics of study participants.

| Parameter | NC | CI | | | p-value |
		MCI	AD		
Total number of participants (N)	264	109	67		
Huashan Hospital (N)	39	30	19		
Prince of Wales Hospital (N)	216	62	31		
Ningxia Medical University (N)	9	17	17		
Age, years (mean (s.d.))	72.62 (5.35)	73.53 (5.38)	73.42 (5.65)		0.256[a]
Education, years (mean (s.d.))	9.88 (4.33)	8.27 (4.80)	8.45 (5.27)		**0.003**[**][a]
Gender, male (N (%))	79 (29.92%)	37 (33.94%)	18 (26.87%)		0.586[b]
Hypertension (N (%))	138 (52.27%)	49 (44.95%)	24 (35.82%)		**0.042**[*][b]
Diabetes (N (%))	50 (18.94%)	24 (22.02%)	9 (13.43%)		0.368[b]
MoCA score (mean (s.d.))	25.55 (3.12)	19.84 (4.50)	12.67 (5.64)		**<0.001**[***][a]
MMSE score (mean (s.d.))	28.71 (1.25)	25.40 (2.70)	16.28 (5.47)		**<0.001**[***][a]

[a]Student's *t*-test for continuous clinical variables (age, education, MoCA score, MMSE score).
[b]Chi-squared test for categorical clinical variables (gender, hypertension, diabetes).
*$p < 0.05$; **$p < 0.01$; ***$p < 0.001$. All statistical tests are performed between NC and CI.

the right eye significantly decreased in the CI group. These findings indicate unique changes in arterial and venous retinal vasculature compared to the overall vasculature. Additionally, the left and right eyes exhibited unique differences despite overall features not showing significant changes between the left and right eyes. Full ANCOVA results for the left and right eyes are provided in Tables S1 and S2, respectively.

In Zone B of the fundus images, the CI group showed a significant reduction in the total length of vessels (zb_len, Figure 3A) and veins (zb_lenV, Figure 3B) in the right eye, indicating a shortening of the retinal vascular network. Additionally, the number of effective vascular segments (zb_num, Figure 3C) and the number of effective venous segments (zb_numV, Figure 3D) significantly decreased for the right eye. In contrast, the average width of vessels (zb_width, Figure 3E) significantly increased. Interestingly, all significant changes identified in Zone B were only found in the right eye; although the left eye exhibited similar trends, the changes were not statistically significant.

In Zone C of the fundus images, the CI group demonstrated significant, though less pronounced, changes in retinal vascular features compared to Zone B (Figure 4A and 4B). For the right eye, the CI group exhibited significant reductions in the total length of vessels (zc_len, Figure 3F) and the number of effective venous segments (zc_numV, Figure 3I). In the left eye, there was a significant reduction in the total length of arteries (zc_lenA, Figure 3G). Additionally, both eyes showed significant reductions in the total length of veins in the CI group (zc_lenV, Figure 3H). Conversely, the average width of vessels in Zone C (zc_width, Figure 3E) significantly increased for both eyes. Notably, when looking at both left and right eyes, the only zone-specific vascular features with significant changes were total length of veins and average width of vessels (zc_lenV and zc_width) (Figure 3H and 3J).

Overall, the 15 combined significant features have moderate correlation and form approximately five clusters with higher correlation (Figure 4A and 4B). These clusters were relatively consistent between the left and right eyes, with related vascular features grouped together, suggesting a systemic pattern in vascular alterations associated with cognitive impairment. The most significant and robust features in the CI group included decreased total length of venous vessels and density of venous vessels for the left eye (skeleton_lenV, densityV) (Figure 4C) and decreased total length of venous vessels and total number of venous bifurcation points for the right eye (skeleton_lenV, n_crossV) (Figure 4D). Similarly, the features with the largest effect sizes included decreased total length of venous vessels (skeleton_lenV, $\eta_p^2 = 0.041$) and density of venous vessels (densityV, $\eta_p^2 = 0.032$) for the left eye and decreased total length of venous vessels (skeleton_lenV, $\eta_p^2 = 0.039$) and total number of venous bifurcation points (n_crossV, $\eta_p^2 = 0.029$) for the right eye (Table S1 and S2).

3.3 | Association between retinal vascular features and cognitive performance

We explored the relationship between retinal vascular features and cognitive performance using regression analyses adjusted for age, education, gender, hypertension, and diabetes. The analyses revealed significant associations between several retinal vascular features, particularly venous structure and complexity, and cognitive performance, as measured by Montreal Cognitive Assessment (MoCA) scores (Figure 5B).

After FDR adjustment, three vascular features showed a significant inverse relationship with cognitive function, while eight features demonstrated a significant direct relationship (-value < 0.1). A higher
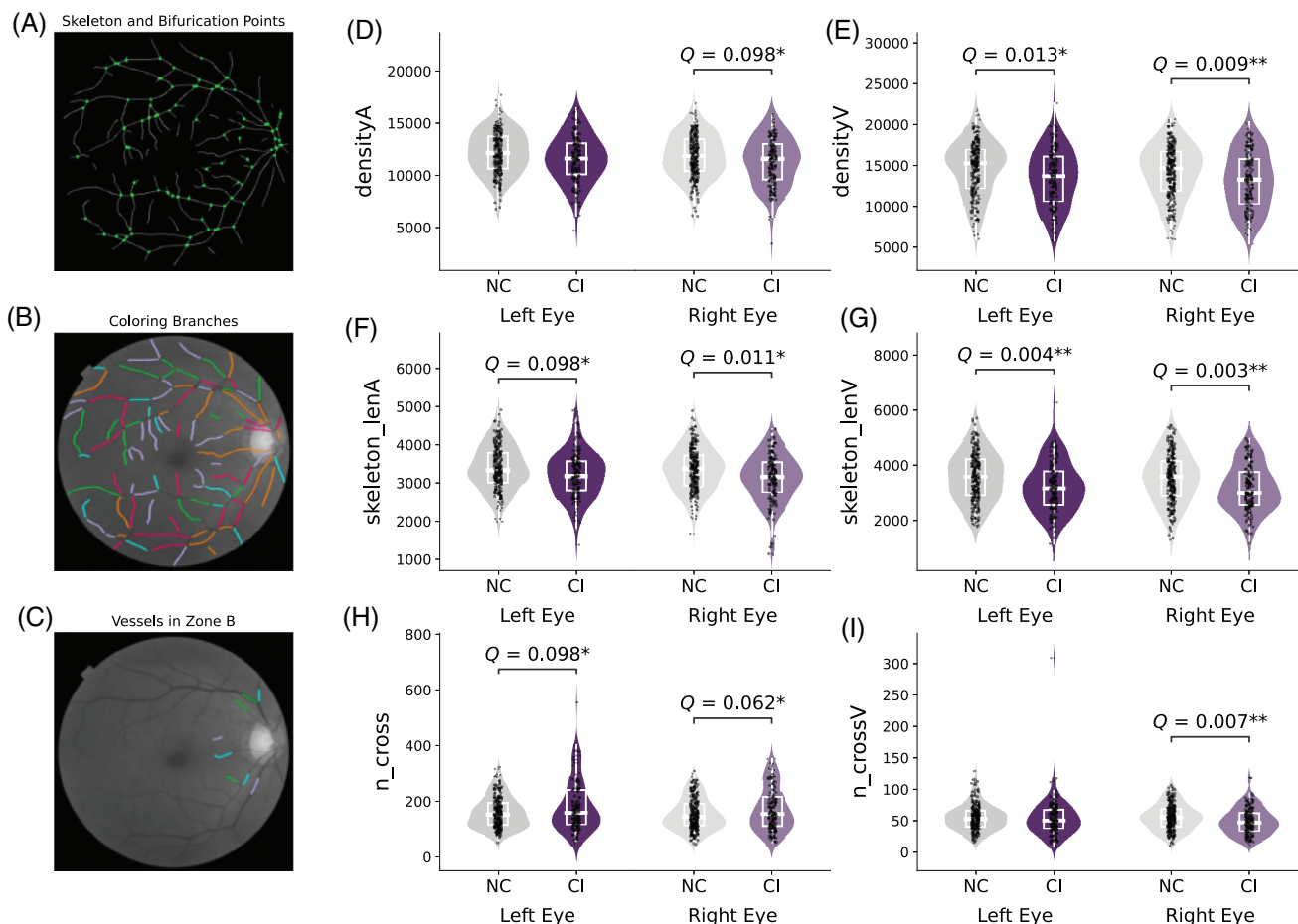
FIGURE 2 Comparison of data distribution of overall retinal vascular features showing significant changes. (A) Schematic diagram of the vascular skeleton (gray) and crossing points (green) in a processed fundus image. (B) Schematic diagram showing the differentiation of each vascular segment in the vascular skeleton and the calculation of the mean width of each segment. (C) Schematic diagram showing the differentiation of each vascular segment in the vascular skeleton in Zone B. DensityA (C), densityV (D), skeleton_lenA (E), and skeleton_lenV (F) decreased significantly in the CI group compared to the NC group. n_cross (H) in both eyes increased significantly in the CI group compared to the NC group. n_crossV (I) for the right eye decreased significantly in the CI group compared to the NC group. Data are presented using violin plots and box plots with median (line) and quartiles (box). ANCOVA p-values adjusted for FDR are reported as Q-values: *$Q < 0.1$; ** $Q < 0.01$; *** $Q < 0.001$.

number of vascular bifurcation points (n_cross, Left $\beta = -0.191$, Right $\beta = -0.131$) correlated with lower cognitive function, while increased venous density (densityV, Left $\beta = +0.212$, Right $\beta = +0.158$) and venous length (skeleton_lenV, Left $\beta = +0.192$, Right $\beta = +0.180$) were linked to better cognitive function. In addition, vessel width in specific zones was associated with cognitive decline, with wider vessels in Zone C (zc_width, Right $\beta = -0.167$) and Zone B (zb_width, Right $\beta = -0.129$) of the right eye correlating with poorer cognitive performance. Notably, although more retinal vascular bifurcation points (n_cross) were correlated with lower cognitive performance, more retinal venous bifurcation points (n_crossV, Right $\beta = +0.156$) were correlated with better cognitive performance. This implies there exist unique changes in arterial and venous retinal vasculature compared to the overall vasculature. Together, the results suggest that retinal vascular alterations are not only present in cognitively impaired individuals but are also correlated with the degree of cognitive dysfunction. Full MoCA score regression results for the left and right eyes are provided in Tables S3 and S4, respectively.

3.4 | Significant differences between groups stratified by cognitive performance

Since retinal vascular features were correlated with the degree of cognitive dysfunction in both regression analyses, we compared patients stratified by MoCA score into NC, MCI, and SD. ANCOVA analysis revealed graded changes from NC to MCI to SD, indicating significant progressive alterations in vascular structure (Figure 6). For instance, the density of veins (densityV) shows significant reductions from NC to SD, with MCI displaying intermediate values (Figure 6A). Notably, the total number of bifurcation points (n_cross) was significantly higher in SD compared to both MCI and NC, suggesting specific vascular changes distinct to SD (Figure 6B). The remaining significant differences are consistent with those identified when comparing only NC and CI (Figure 6C–I). Taken together, these findings underscore the potential of retinal vascular metrics as biomarkers for detection and monitoring of cognitive impairment level.
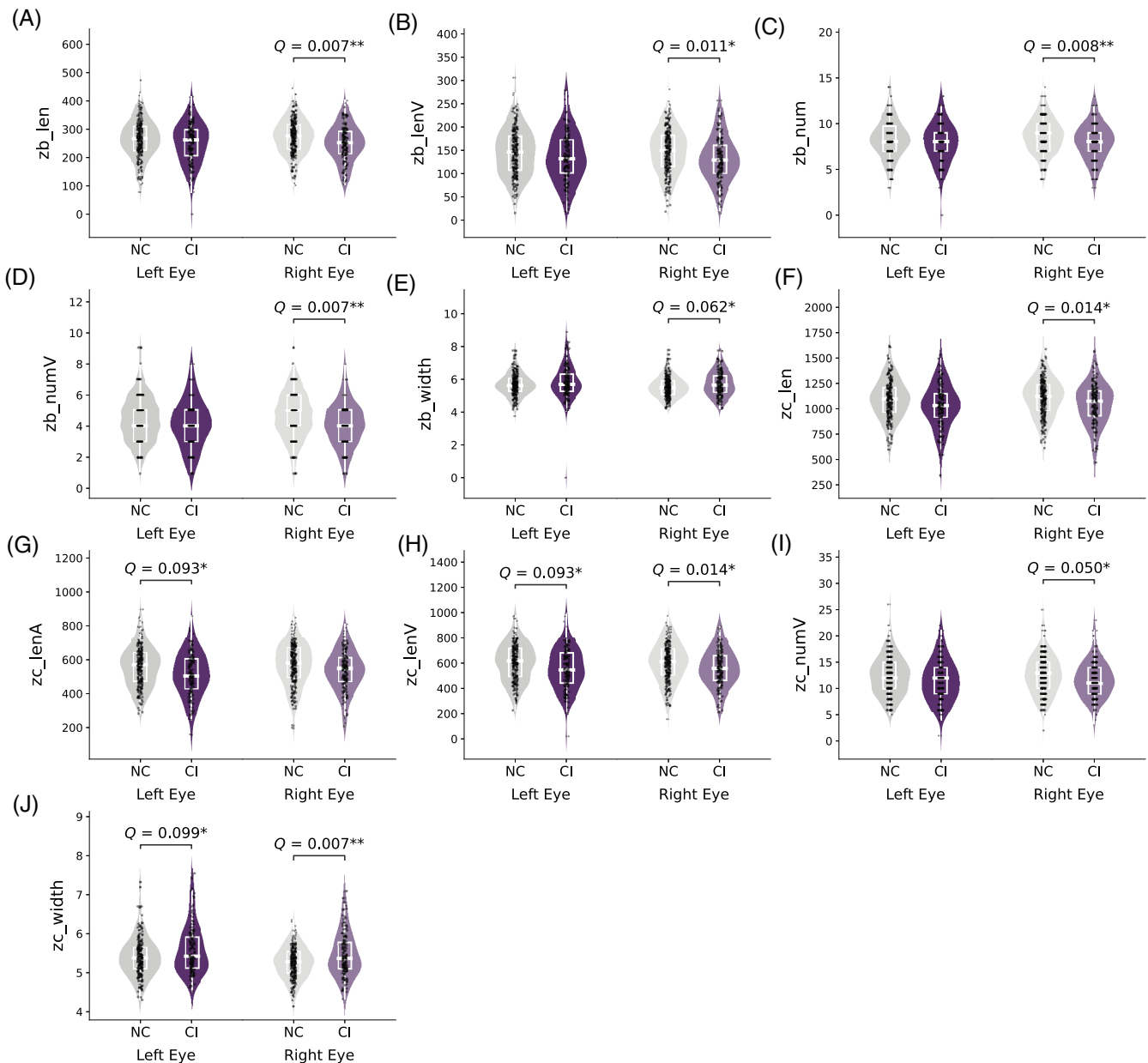
FIGURE 3 Comparison of data distribution of retinal vascular features with significant changes in Zone B and Zone C. For Zone B, zb_len (A), zb_lenV (B), zb_num (C), and zb_numV (D) for the right eye decreased significantly in the CI group compared to the NC group while zb_width (E) for the right eye increased significantly. For Zone C, zc_len (F), zc_lenA (G), zc_lenV (H), and zc_numV (I) in some eyes decreased significantly in the CI group compared to the NC group while zc_width (J) for both eyes increased significantly. Data are presented using violin plots and box plots with median (line) and quartiles (box). ANCOVA p-values adjusted for FDR are reported as Q-values: *$Q < 0.1$; **$Q < 0.01$; ***$Q < 0.001$.

3.5 | Classification performance of retinal vascular features

Finally, using the significant retinal vascular features identified, we conducted classification analyses to evaluate their effectiveness in distinguishing between NC and CI individuals with logistic regression, SVM, and random forest models. The models were trained using different sets of features: demographics alone, significant vascular features alone, a combination of demographics and vascular features, DINOv2 features alone, and a combination of demographics and

DINOv2 features (Table S5). The DINOv2 features offer a point of comparison for our extracted vascular features to non-interpretable deep-learning features extracted directly from fundus photographs via self-supervised learning.

The five-fold cross-validation results demonstrate that models utilizing significant vascular features alone outperform those utilizing demographics alone across all metrics and model types (Figure 5C, 5D, and 5E). The logistic regression model utilizing significant vascular features alone achieved an accuracy of 62.11% ± 3.61%, AUC of 0.642 ± 0.030, and a Brier score of 0.231 ± 0.010, outperform-
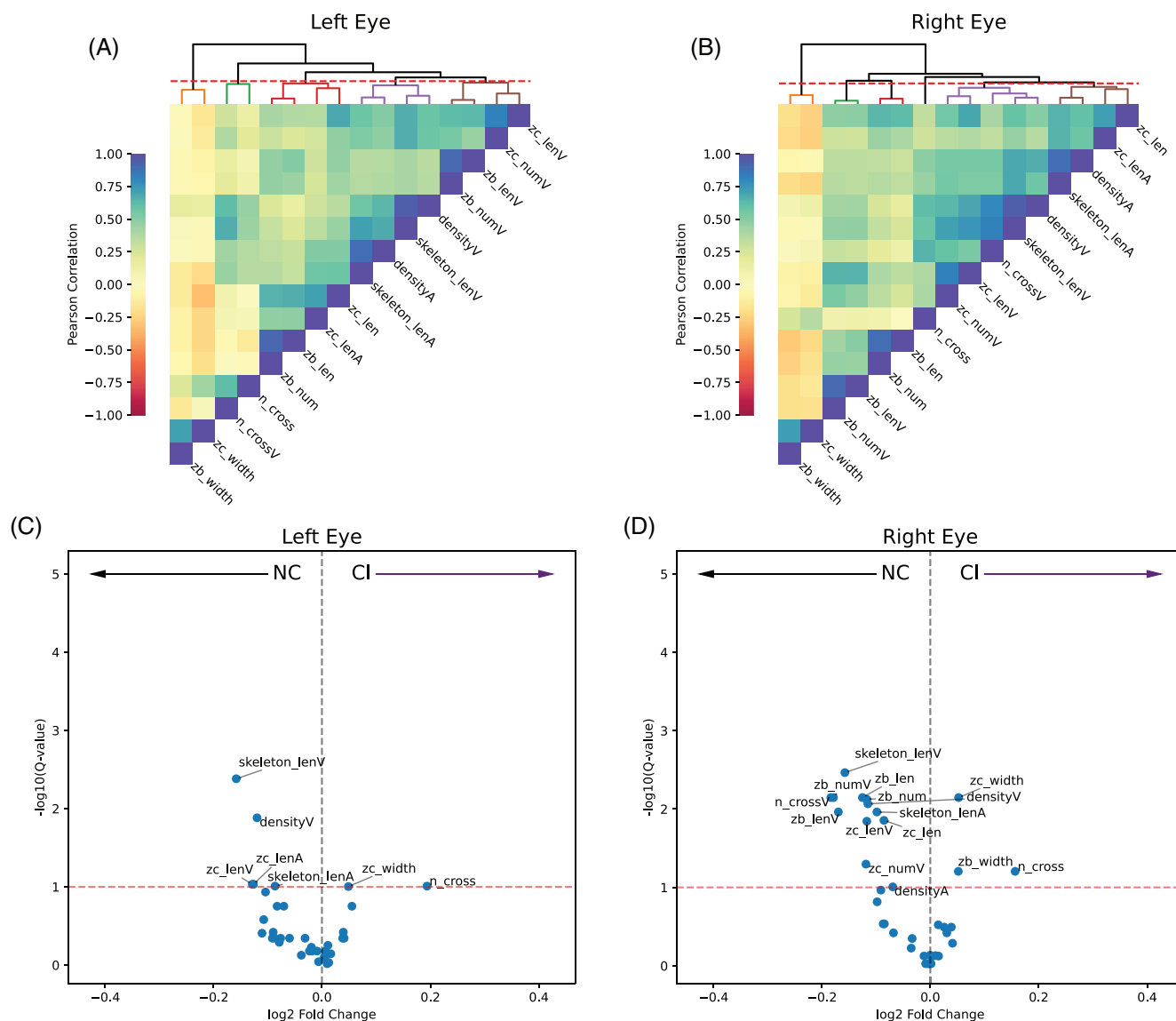
FIGURE 4 Significantly different vascular features in the left and right eyes. Heatmaps depict the pairwise Pearson correlation between extracted vascular features with significant differences in both eyes for the left (A) or right (B) eyes. Features are hierarchically clustered and a dendrogram with cutoff at 1 for clustering is shown. Volcano plots show the significance and magnitude of change in the extracted vascular features for the left (C) and right (D) eyes separately. The red dotted line indicates an FDR cutoff of 0.1, with features elevated in the CI group compared to the NC group further to the right (positive logFC).

ing the demographics-only model (accuracy: 59.87% ± 3.29%; AUC: 0.625 ± 0.036; Brier score: 0.239 ± 0.009). Incorporating both demographics and vascular features yielded a slight improvement suggesting complementary information between these feature sets. The SVM model showed comparable performance using vascular features alone and when combined with demographics, the SVM model's accuracy improved to 63.34% ± 1.14%. Notably, the SVM model incorporating DINOv2 features demonstrated higher accuracy (67.31% ± 3.24%) and AUC (0.695 ± 0.042), suggesting that deep learning features capture additional information relevant to cognitive impairment. The random forest model exhibited the highest classification performance among the tested models. Using vascular features alone, it achieved an accuracy of 65.99% ± 2.17% and an AUC of 0.634 ± 0.038, outperform-

ing the demographics-only model (accuracy: 63.62% ± 1.82%; AUC: 0.647 ± 0.040). Combining demographics and vascular features led to the highest accuracy model tested (accuracy: 69.40% ± 2.44%), indicating that vascular features provide additive diagnostic value. These results suggest that the identified retinal vascular features may be useful for identifying cognitive impairment. Full metrics for classification performance are provided in Table S5.

4 | DISCUSSION

Our analysis examined retinal vascular features from both the left and right eyes, extracted using a deep learning model, focusing on Zones
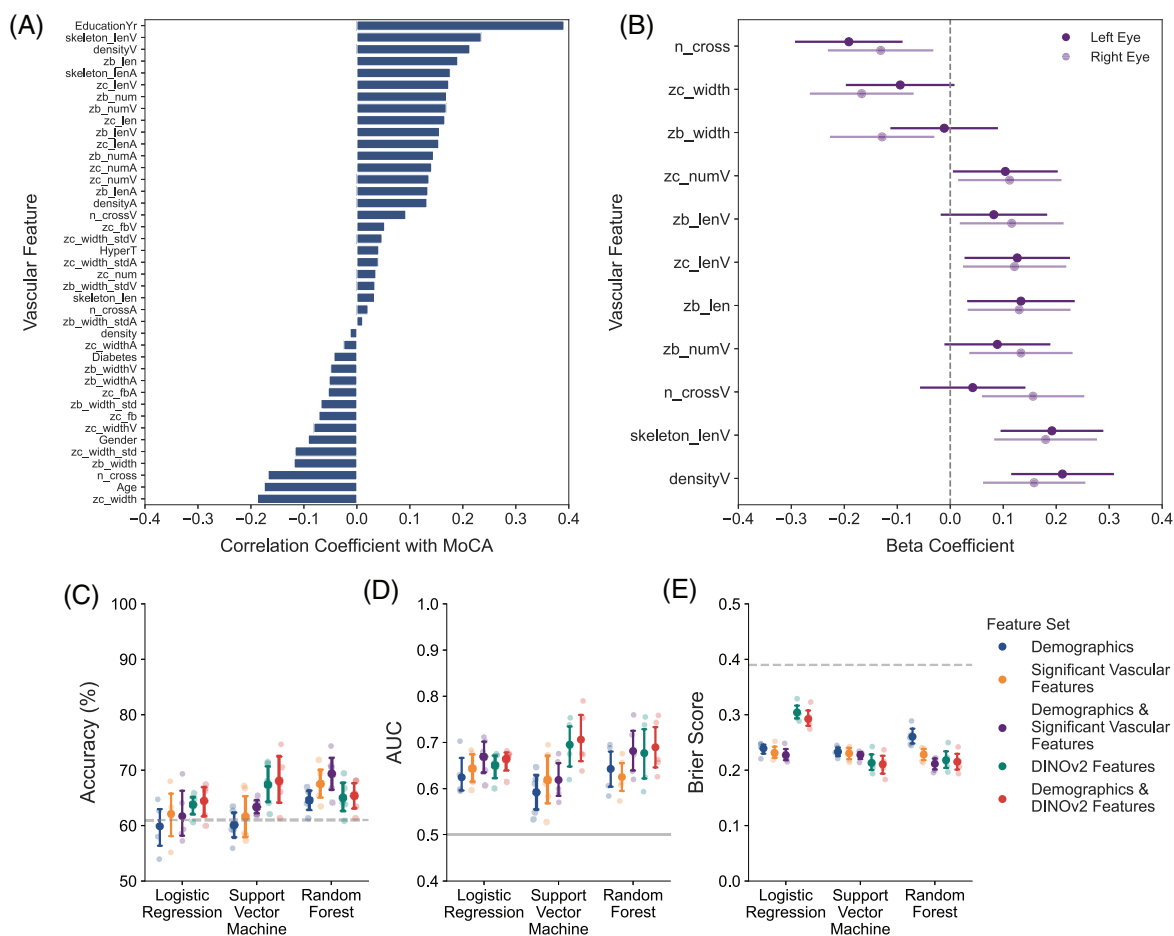
FIGURE 5 Correlation of vascular features with cognitive performance and classification results of NC and CI. (A) Bar plot of Pearson correlation coefficients between each feature (demographic and vascular) and MoCA scores. (B) Forest plot of beta coefficients of GLM regression models, demographics and one additional vascular feature, assessing their association with MoCA scores. Only models where the Q-value of the vascular feature coefficient is less than 0.1 are included. The forest plot shows each regressors' standardized beta coefficient, with 95% confidence interval, enabling the effect size of variables to be compared. Five-fold cross-validation results for classification between NC and CI are reported as mean (C) accuracy, (D) AUC, and (E) Brier score with 95% error bars. Performance metrics are compared across models (logistic regression, SVM, and random Forest) and different feature sets (legend right). The dotted gray line indicates the performance of a dummy classifier that always guesses the majority class (NC).

B and C. The CI group exhibited statistically significant changes compared to the NC group among several vascular features. Specifically, compared to NC, patients with CI showed significant changes in total length, bifurcation points, and vascular width of arteries and veins in both Zones B and C. These findings suggest that structural changes in retinal vessel segments may play a role in early cognitive decline.

Overall, the CI group exhibited a significant increase in number of bifurcation points and decrease in total vessel length, which may reflect an adaptive mechanism or pathological change in the local microvasculature. The increased bifurcation points may reflect a compensatory response to inadequate blood supply by increasing vessel branching to maintain normal brain function. Notably, the number of bifurcation points is one of only two features that increase in the CI group for both eyes. On the other hand, the reduction in vessel lengths could indicate microvascular rarefaction or loss, commonly associated with microvascular pathology and local hypoperfusion.[39] Furthermore, both venous and arterial densities significantly decreased in the CI

group. The reduction in venous density could indicate venous dilation, blood flow stasis, and microvascular pathology, which are associated with neurodegenerative diseases and cognitive decline. The decrease in arterial density may reflect arteriosclerosis, vascular narrowing, or reduced perfusion capacity, which would affect brain blood supply and contribute to cognitive decline.[40]

Stratifying patients by MoCA scores revealed graded changes in some features from NC to MCI to SD. This suggests existing underlying mechanisms may drive progressive alterations in vascular structure that change along with cognition. However, the total number of bifurcation points significantly increased only in SD, suggesting specific vascular changes distinct to dementia. While graded changes in vascular features may correlate with general cognitive decline, features unique to SD are likely driven by more extensive neurodegeneration. Increased bifurcation points could signify an attempt to maintain adequate blood supply and compensate for degeneration in the local microvasculature that does not occur in MCI.
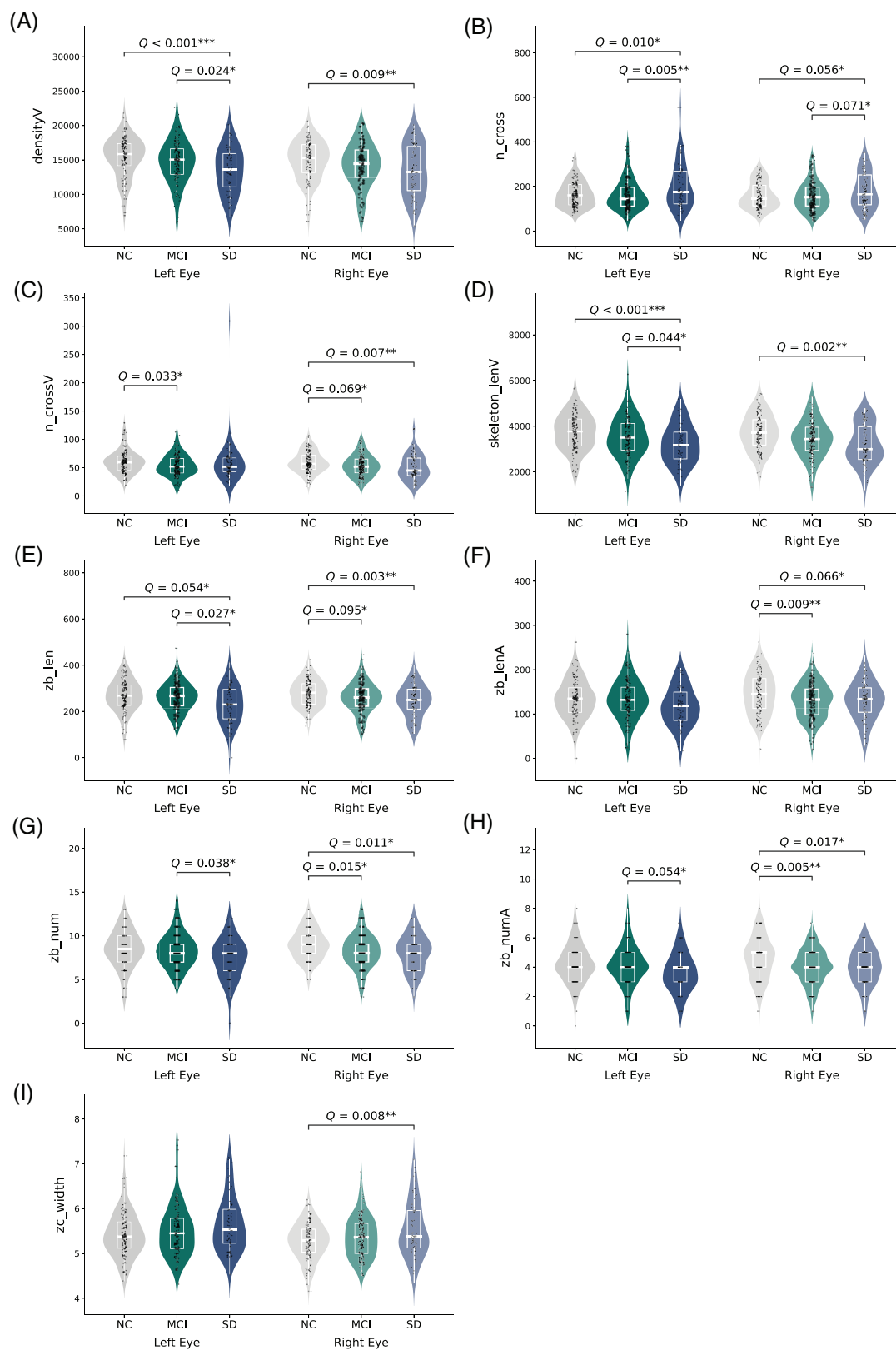
FIGURE 6 Comparison of data distribution of retinal vascular features with significant changes in NC, MCI, or SD groups. Statistically significant differences were found in at least one pairwise comparison for densityV (A), n_cross (B), n_crossV (C), skeleton_lenV (D), zb_len (E), zb_lenA (F), zb_num (G), zb_numA (H), zc_width (I). Data are presented using violin plots and box plots with median (line) and quartiles (box). ANCOVA Tukey post-hoc *p*-values adjusted for FDR are reported as Q-values: *Q < 0.1; **Q < 0.01; ***Q < 0.001.

While the overall changes were largely significant in both eyes, region-specific features were more frequently significant in the right eye (15 vs. 7 in the left). The reason for this asymmetry is unclear and may simply be due to data variations or potentially fundamental physiological differences between the eyes. This is entirely possible as researchers have found accelerated asymmetric cortical thinning in AD and retinal asymmetry in macular layer thickness in Multiple Sclerosis.[41,42] Nonetheless, both eyes typically exhibited the same trends, even if one did not reach statistical significance.

In Zone B, statistically significant features included a decrease in total length of vessels and number of effective segments. These changes were exclusively observed in venous features, with none detected in arterial ones. Moreover, there were only three arterial related features compared to seven venous related features across all zones. This suggests venous changes may be more sensitive indicators of cognitive decline in Zone B. Additionally, the reduction in vessel length and the number of effective segments could indicate a compromised venous network, potentially leading to hypoperfusion and subsequent neurodegeneration characteristic of AD.[43,44]

In Zone C, we mainly observed significant reductions in the length of overall, venous, and arterial retinal vessels. This indicates a generalized shortening of the vascular network within this zone associated with cognitive impairment. Moreover, Zone C exhibited significant changes in both eyes. Specifically, the total length of vessels and average width of vessels were the only zone-specific features showing significant alterations bilaterally. This consistency suggests these features may serve as robust biomarkers for detecting vascular changes linked to cognitive decline. Finally, the only feature that significantly increased in both Zone B and Zone C was average vessel width. An increase in vessel width may be associated with structural damage to small vessels, leading to reduced blood flow, hypoperfusion, and inflammation, which can contribute to neuronal damage and cognitive decline.[43]

Our study further demonstrated that retinal vascular features are not only altered in CI individuals but also correlate with the degree of cognitive decline. Regression analyses revealed that decreased venous density and length, as well as increased vessel width and number of bifurcation points, were significantly correlated with lower MoCA scores. Notably, out of the 11 significant coefficients 7 were venous features, with no arterial ones. Again, this suggests venous changes may better explain changes in cognitive function.

In terms of classification, models trained on significant vascular features alone outperformed models trained on demographics alone across all models and metrics, indicating their potential utility in distinguishing CI individuals. Although the improvements in classification were modest at best, they were monotonic in nature and consistently highlighted the additive diagnostic value of vascular features. In fact, the performance of models utilizing only 16 significant vascular features were comparable and sometimes even superior to those utilizing 768 non-interpretable deep-learning features from DINOv2. Thus, retinal vascular features could potentially add useful information to a practical, non-invasive tool for identifying cognitive impairment.

Recently, several deep-learning models have been reported for detecting AD using retinal imaging techniques (Table S6). Among them,

Eye-AD achieved an AUC of 0.90 for early AD and 0.80 for MCI detection using 5751 OCTA images.[45] Similarly, Cheung et al. developed a model using 12,949 retinal fundus photographs that could classify AD with 83.6% accuracy and an AUC of 0.93.[22] While previous studies such as these report markedly higher accuracies, they were all trained on larger-sampled datasets and generally lacked interpretability. In contrast, our approach prioritizes interpretability by extracting physiologically meaningful vascular features altered in cognitive impairment. Our relatively modest performance can be attributed to the relatively small sample size, the absence of AD-specific biomarkers for well-defined groups, and our focus on interpretability. Still, our baseline deep learning approach (DINOv2) yielded similar accuracy, suggesting data constraints rather than model choice are likely limiting performance.

Overall, these results underscore the potential specificity of vascular structural changes as early indicators of cognitive impairment. The current AD diagnostic framework, AT(N), is adaptable, allowing for the inclusion of new biomarkers in the existing three groups and adding new biomarker categories as they emerge.[46] Although retinal vascular biomarkers are promising due to their economic affordability and clinical accessibility, their application to AD diagnostics is subject to scrutiny due to mixed research results.[47,48] Our findings suggest potential regional differences in structural changes of specific retinal vascular features. Future research of retinal vasculature should pay close attention to possible differences in different areas or dimensions of the retinal fundus and potential asymmetries between eyes. While the potential specificity of changes in vessel length and density is promising, it should be integrated into a comprehensive diagnostic framework that considers multiple factors and markers.

Progress in explainable artificial intelligence (AI) emphasizes the importance of interpretable models, particularly in medical diagnostics.[49] Developing interpretable models is important because they provide transparency and trust vital for clinical acceptance and integration into patient care.[50,51] Here, by identifying statistically significant retinal vascular features associated with cognitive impairment using a deep learning segmentation model, we provide clear, quantifiable changes in retinal vasculature that may guide the development of interpretable models for early diagnosis and monitoring of cognitive decline.

This study has several limitations. Despite our efforts to collect data from multiple medical centers, we faced limitations due to clinical data availability. Importantly, we did not use AD-specific biomarkers (e.g., PET imaging, CSF, or plasma p-tau) to confirm AD pathology in our participants. As such, we cannot attribute the observed retinal vascular changes specifically to AD. Future studies incorporating AD-specific biomarkers are necessary to determine whether these changes are specific to AD or are indicative of cognitive impairment more broadly. Additionally, considerable overlap between AD and age-related eye diseases or cerebrovascular diseases is expected, as these conditions often co-occur due to shared risk factors.[22,52] Although we excluded participants with concomitant eye diseases, we did not account for concomitant cerebrovascular diseases due to lack of access to such clinical information. Some of the recruited patients from Prince of Wales Hos-

pital had small vessel disease, which may have been a confounding factor in our results. Finally, only one-third of the retinal features showed differences between NC and MCI. This suggests that while most retinal features might be useful in identifying more advanced stages of cognitive impairment, their effectiveness in detecting early-stage impairment remains unclear. Further investigation with larger sample sizes is needed to determine the sensitivity of these features for early-stage detection and to establish the necessity of retinal image features as a screening tool in the community population.

In conclusion, the potential specificity of retinal vascular structural changes in CI individuals found in our study contributes to the growing body of knowledge on the potential of retinal vascular features as biomarkers for cognitive impairment. Further studies and clinical validations are needed to fully understand the utility of these markers and their role in clinical practice, which may lead to the development of novel interpretable models for identifying or monitoring cognitive decline.

AUTHOR CONTRIBUTION

Jiayi Zhang, Timonthy Kwok, Qianhua Zhao, Qin Shi, and Biao Yan conceptualized, designed, and supervised this study. Jiayi Zhang, Qin Shi, Qianhua Zhao, and Biao Yan acquired funding for this study. Timothy Kwok, Zhenxu Xiao, Wanqing Wu, Peijun Zhang, Ding Ding, Mingxuan Wang, Kaiwen Shi, and Qianhua Zhao collected data. Wenbin Xie, Mingxuan Wang, Kaiwen Shi, Kexin Li, and Andrew Ni trained and modified the computational models. Andrew Ni, Kexin Li, Wenxin Su, and Wenbin Xie analyzed data. Andrew Ni, Kexin Li,Hao Zheng, and Wenxin Su interpreted data. Kexin Li wrote the original draft. Andrew Ni, Kexin Li, Qin Shi, and Jiayi Zhang revised and edited the manuscript with valuable input from all authors.

CONFLICT OF INTEREST STATEMENT

None declared. Author disclosures are available in the supporting information.

DATA AVAILABILITY STATEMENT

Data except patient identification are available upon reasonable request to the corresponding author Dr. Jiayi Zhang.

ETHICS APPROVAL AND CONSENT

The study was approved by Joint Chinese University of Hong Kong-New Territories East Cluster Clinical Research Ethics Committee, General Hospital of Ningxia Medical University, and the Medical Ethics Committee of Huashan Hospital, Fudan University, Shanghai. Informed consent was acquired from all participants.

ORCID

Timothy Kwok https://orcid.org/0000-0001-9253-3549

REFERENCES

1. Arvanitakis Z, Shah RC, Bennett DA. Diagnosis and Management of Dementia: Review. *Jama.* 2019;322(16):1589-1599. doi:10.1001/jama.2019.4782
2. Polanco JC, Li C, Bodea LG, Martinez-Marmol R, Meunier FA, Götz J. Amyloid-β and tau complexity - towards improved biomarkers and targeted therapies. *Nat Rev Neurol.* 2018;14(1):22-39. doi:10.1038/nrneurol.2017.162
3. 2022 Alzheimer's disease facts and figures. *Alzheimer's & Dementia.* 2022;18(4):700-789. doi:10.1002/alz.12638
4. Bartels C, Kögel A, Schweda M, et al. Use of Cerebrospinal Fluid Biomarkers of Alzheimer's Disease Risk in Mild Cognitive Impairment and Subjective Cognitive Decline in Routine Clinical Care in Germany. *J Alzheimers Dis.* 2020;78(3):1137-1148. doi:10.3233/jad-200794
5. Gauthier S WC, Servaes S, Morais JA, Rosa-Neto P. World Alzheimer Report 2022: Life after diagnosis: Navigating treatment, care and support. 2022.
6. Dementia warning for the Asia-Pacific region. *Lancet Neurol.* 2015;14(1):1. doi:10.1016/S1474-4422(14)70312-6
7. Ho PC, Yu WH, Tee BL, et al. Asian Cohort for Alzheimer's Disease (ACAD) pilot study on genetic and non-genetic risk factors for Alzheimer's disease among Asian Americans and Canadians. *Alzheimers Dement.* 2024;20(3):2058-2071. doi:10.1002/alz.13611
8. Lim AC, Barnes LL, Weissberger GH, et al. Quantification of race/ethnicity representation in Alzheimer's disease neuroimaging research in the USA: a systematic review. *Commun Med (Lond).* 2023;3(1):101. doi:10.1038/s43856-023-00333-6
9. 2023 Alzheimer's disease facts and figures. *Alzheimer's & Dementia.* 2023;19(4):1598-1695. doi:10.1002/alz.13016
10. Cheung CY, Mok V, Foster PJ, Trucco E, Chen C, Wong TY. Retinal imaging in Alzheimer's disease. *J Neurol Neurosurg Psychiatry.* 2021;92(9):983-994. doi:10.1136/jnnp-2020-325347
11. London A, Benhar I, Schwartz M. The retina as a window to the brain-from eye research to CNS disorders. *Nat Rev Neurol.* 2013;9(1):44-53. doi:10.1038/nrneurol.2012.227
12. Apte RS. Retinal Imaging as a Predictor of Cognitive Impairment. *JAMA Ophthalmol.* 2022;140(7):691. doi:10.1001/jamaophthalmol.2022.1721
13. Szegedi S, Dal-Bianco P, Stögmann E, et al. Anatomical and functional changes in the retina in patients with Alzheimer's disease and mild cognitive impairment. *Acta Ophthalmol. Nov* 2020;98(7):e914-e921. doi:10.1111/aos.14419
14. Asanad S, Fantini M, Sultan W, et al. Retinal nerve fiber layer thickness predicts CSF amyloid/tau before cognitive decline. *PLoS One.* 2020;15(5):e0232785. doi:10.1371/journal.pone.0232785
15. Ge YJ, Xu W, Ou YN, et al. Retinal biomarkers in Alzheimer's disease and mild cognitive impairment: A systematic review and meta-analysis. *Ageing Res Rev.* 2021;69:101361. doi:10.1016/j.arr.2021.101361
16. Abraham AG, Guo X, Arsiwala LT, et al. Cognitive decline in older adults: What can we learn from optical coherence tomography (OCT)-based retinal vascular imaging? *J Am Geriatr Soc.* 2021;69(9):2524-2535. doi:10.1111/jgs.17272
17. Moussa M, Falfoul Y, Nasri A, et al. Optical coherence tomography and angiography in Alzheimer's disease and other cognitive disorders. *Eur J Ophthalmol.* 2023;33(4):1706-1717. doi:10.1177/11206721221148952

18. Wu J, Zhang X, Azhati G, Li T, Xu G, Liu F. Retinal microvascular attenuation in mental cognitive impairment and Alzheimer's disease by optical coherence tomography angiography. *Acta Ophthalmol.* 2020;98(6):e781-e787. doi:10.1111/aos.14381

19. Lee CS, Larson EB, Gibbons LE, et al. Associations between recent and established ophthalmic conditions and risk of Alzheimer's disease. *Alzheimers Dement.* 2019;15(1):34-41. doi:10.1016/j.jalz.2018.06.2856

20. Kumar V, Surve A, Kumawat D, et al. Ultra-wide field retinal imaging: A wider clinical perspective. *Indian J Ophthalmol.* 2021;69(4):824-835. doi:10.4103/ijo.IJO_1403_20

21. Jayanna S, Padhi TR, Nedhina EK, Agarwal K, Jalali S. Color fundus imaging in retinopathy of prematurity screening: Present and future. *Indian J Ophthalmol.* 2023;71(5):1777-1782. doi:10.4103/ijo.Ijo_2913_22

22. Cheung CY, Ran AR, Wang S, et al. A deep learning model for detection of Alzheimer's disease based on retinal photographs: a retrospective, multicentre case-control study. *The Lancet Digital Health.* 2022;4(11):e806-e815. doi:10.1016/S2589-7500(22)00169-8

23. Zhou Y, Chia MA, Wagner SK, et al. A foundation model for generalizable disease detection from retinal images. *Nature.* 2023;622(7981):156-163. doi:10.1038/s41586-023-06555-x

24. American Psychiatric Association. *Diagnostic and Statistical Manual of Mental Disorders*, ed 4. Washington, DC: American Psychiatric Association; 1994:143-147.

25. McKhann G, Drachman D, Folstein M, Katzman R, Price D, Stadlan EM. Clinical diagnosis of Alzheimer's disease: report of the NINCDS-ADRDA Work Group under the auspices of Department of Health and Human Services Task Force on Alzheimer's Disease. *Neurology.* 1984;34(7):939-944. doi:10.1212/wnl.34.7.939

26. Petersen RC. Mild cognitive impairment as a diagnostic entity. *J Intern Med.* 2004;25(2):183-194. doi:10.1111/j.1365-2796.2004.01388.x

27. Blacker D, Albert MS, Bassett SS, Go RC, Harrell LE, Folstein MF. Reliability and validity of NINCDS-ADRDA criteria for Alzheimer's disease. The National Institute of Mental Health Genetics Initiative. *Arch Neurol.* 1994;51(12):1198-1204. doi:10.1001/archneur.1994.00540240042014

28. Varma AR, Snowden JS, Lloyd JJ, Talbot PR, Mann DM, Neary D. Evaluation of the NINCDS-ADRDA criteria in the differentiation of Alzheimer's disease and frontotemporal dementia. *J Neurol Neurosurg Psychiatry.* 1999;66(2):184-188. doi:10.1136/jnnp.66.2.184

29. Lau QP, Lee ML, Hsu W, Wong TY. Simultaneously identifying all true vessels from segmented retinal images. *IEEE Trans Biomed Eng.* 2013;60(7):1851-1858. doi:10.1109/tbme.2013.2243447

30. Bhuiyan A, Kawasaki R, Lamoureux E, Ramamohanarao K, Wong TY. Retinal artery-vein caliber grading using color fundus imaging. *Computer methods and programs in biomedicine.* 2013;111:104-114. doi:10.1016/j.cmpb.2013.02.004

31. Frost S, Kanagasingam Y, Sohrabi H, et al. Retinal vascular biomarkers for early detection and monitoring of Alzheimer's disease. *Transl Psychiatry.* 2013;3(2):e233. doi:10.1038/tp.2012.150

32. Burlina PM, Joshi N, Pekala M, Pacheco KD, Freund DE, Bressler NM. Automated Grading of Age-Related Macular Degeneration From Color Fundus Images Using Deep Convolutional Neural Networks. *JAMA Ophthalmol.* 2017;135(11):1170-1176. doi:10.1001/jamaophthalmol.2017.3782

33. Hu J, Wang H, Cao Z, et al. Automatic Artery/Vein Classification Using a Vessel-Constraint Network for Multicenter Fundus Images. *Front Cell Dev Biol.* 2021;9:659941. doi:10.3389/fcell.2021.659941

34. Gulshan V, Peng L, Coram M, et al. Development and Validation of a Deep Learning Algorithm for Detection of Diabetic Retinopathy in Retinal Fundus Photographs. *Jama.* 2016;316(22):2402-2410. doi:10.1001/jama.2016.17216

35. Jia X, Wang Z, Huang F, et al. A comparison of the Mini-Mental State Examination (MMSE) with the Montreal Cognitive Assessment (MoCA) for mild cognitive impairment screening in Chinese middle-aged and older population: a cross-sectional study. *BMC Psychiatry.* 2021;21(1):485. doi:10.1186/s12888-021-03495-6

36. Pinto TCC, Machado L, Bulgacov TM, et al. Is the Montreal Cognitive Assessment (MoCA) screening superior to the Mini-Mental State Examination (MMSE) in the detection of mild cognitive impairment (MCI) and Alzheimer's Disease (AD) in the elderly?. *Int Psychogeriatr.* 2019;31(4):491-504. doi:10.1017/S1041610218001370

37. Oquab M, Darcet T, Moutakanni T, et al. DINOv2: Learning Robust Visual Features without Supervision. arXiv.org. https://arxiv.org/abs/2304.07193

38. Dosovitskiy A, Beyer L, Kolesnikov A, et al. An Image is Worth 16×16 Words: Transformers for Image Recognition at Scale. arXiv:201011929 [cs]. https://arxiv.org/abs/2010.11929

39. van Dinther M, Bennett J, Thornton GD, et al. Evaluation of microvascular rarefaction in vascular cognitive impairment and heart failure (CRUCIAL): Study protocol for an observational study. *Cerebrovasc Dis Extra.* 2023;13(1):18-32. doi:10.1159/000529067

40. Meissner MH, Moneta G, Burnand K, Gloviczki P, Lohr JM, Lurie F, Mattos MA, McLafferty RB, Mozes G, Rutherford RB, Padberg F, Sumner DS. The hemodynamics and diagnosis of venous disease. *J Vasc Surg.* 2007;46(Suppl S):4S-24S. doi:10.1016/j.jvs.2007.09.043

41. Roe JM, Vidal-Piñeiro D, Sørensen Ø, et al. Asymmetric thinning of the cerebral cortex across the adult lifespan is accelerated in Alzheimer's disease. *Nat Commun.* 2021;12(1):721. doi:10.1038/s41467-021-21057-y

42. Petzold A, Chua SYL, Khawaja AP, et al. Retinal asymmetry in multiple sclerosis. *Brain.* 2020;144(1):224-235. doi:10.1093/brain/awaa361

43. Kitamura A, Hase Y, Ihara M, Kalaria RN, Horsburgh K. Chronic cerebral hypoperfusion: a key mechanism leading to vascular cognitive impairment and dementia. *Clin Sci (Lond).* 2017;131(19):2451-2468. doi:10.1042/CS20160727

44. From Chronic Cerebral Hypoperfusion to Alzheimer-Like Brain Pathology and Neurodegeneration. *Cell Mol Neurobiol.* 2021;41(5):797-805. doi:10.1007/s10571-020-00941-8

45. Hao J, Kwapong WR, Shen T, Fu H, Xu Y, Lu Q et al. Early detection of dementia through retinal imaging and trustworthy AI. *npj Digital Medicine.* 2024;7(1):294. doi:10.1038/s41746-024-01292-5

46. Jack CR, Jr., Bennett DA, Blennow K, et al. NIA-AA Research Framework: Toward a biological definition of Alzheimer's disease. *Alzheimers Dement.* 2018;14(4):535-562. doi:10.1016/j.jalz.2018.02.018

47. den Haan J, van de Kreeke JA, van Berckel BN, et al. Is retinal vasculature a biomarker in amyloid proven Alzheimer's disease? *Alzheimers Dement (Amst).* 2019;11:383-391. doi:10.1016/j.dadm.2019.03.006

48. Alber J, Goldfarb D, Thompson LI, et al. Developing retinal biomarkers for the earliest stages of Alzheimer's disease: What we know, what we don't, and how to move forward. *Alzheimers Dement.* 2020;16(1):229-243. doi:10.1002/alz.12006

49. Markus AF, Kors JA, Rijnbeek PR. The role of explainability in creating trustworthy artificial intelligence for health care: A comprehensive survey of the terminology, design choices, and evaluation strategies. *Journal of Biomedical Informatics.* 2021;113:103655. doi:10.1016/j.jbi.2020.103655

50. He J, Baxter SL, Xu J, Xu J, Zhou X, Zhang K. The practical implementation of artificial intelligence technologies in medicine. *Nature Medicine.* 2019;25(1):30-36. doi:10.1038/s41591-018-0307-0

51. Topol EJ. High-performance medicine: the convergence of human and artificial intelligence. *Nature Medicine.* 2019;25(1):44-56. doi:10.1038/s41591-018-0300-7

52. Liew G, Wang JJ, Cheung N, et al. The retinal vasculature as a fractal: methodology, reliability, and relationship to blood pressure. *Oph-

thalmology. 2008;115(11):1951-1956. doi:10.1016/j.ophtha.2008.05.029

SUPPORTING INFORMATION

Additional supporting information can be found online in the Supporting Information section at the end of this article.